Frailty Assessment using HRV During Physical Activity

Saman Parvaneh[1], Sadaf Moharreri[2], Nima Toosizadeh[3], Shahab Rezaei[4]

[1]Edwards Lifesciences, Irvine, California, USA
[2]Department of Biomedical Engineering, Kho.C., Islamic Azad University, Khomeinishahr, Iran
[3]Department of Rehabilitation and Movement Sciences, School of Health Professions, Rutgers University, Newark, New Jersey, USA
[4]Department of Biomedical Engineering, CT.C., Islamic Azad University, Tehran, Iran

Abstract

Studies have shown a strong link between heart rate variability (HRV) and frailty. In this paper, frailty is assessed using HRV during physical activity. This study used a single-lead ECG collected from patients after open-heart surgery during multiple physical activities. Frailty was assessed using the Edmonton Frail Scale (EFS), where scores equal to or lower than five were considered non-frail, and scores greater than five were considered frail. QRS peaks during a 6-minute walk test were detected using the Pan-Tompkins algorithm, followed by the extraction of 36 HRV features. Extracted features include statistical features (e.g., SDNN, pNN50), frequency features (e.g., low and high-frequency power), traditional Poincare features (e.g., SD1 and SD2), geometric Poincare features (e.g., local and global cooccurrence features), and heart rate asymmetry (e.g., Guzik and Porta index). Multiple classifiers were trained for frailty assessment, including a decision tree and a neural network, and the best model was selected via 5-fold cross-validation. ECGs for sixty-seven participants (29 non-frail and 38 frail) were analyzed. A CatBoost Classifier was the best-performing classifier, leading to an F1 score of 84.6% and an AUC of 0.82. Promising results suggest the potential of using HRV during physical activity and machine learning for frailty assessment.

1. Introduction

Frailty is a geriatric syndrome characterized by reduced physiological reserves and heightened vulnerability to stressors [1]. Among older adult patients undergoing major cardiac surgery, frailty is associated with delayed postoperative recovery and an elevated risk of adverse outcomes [2].

Frailty is consistently linked with dysregulation of the autonomic nervous system (ANS) and impaired cardiac autonomic control [3]. This impairment is frequently observed through reduced heart rate variability (HRV) in individuals with higher levels of frailty [3-7]. Recent research suggests that frailty can be more accurately assessed by analyzing cardiovascular responses to physical activity, such as the upper-extremity function test [5, 8, 9]. Studies show that frail older adults often exhibit attenuated heart rate (HR) increases and slower peak HR responses during physical activity or orthostatic challenges, indicating a diminished capacity to physiologically adapt to stress [3, 8]. While resting HRV is a common measure of ANS function, studies suggest that HRV responses to controlled stressors, such as walking or upper-extremity tasks, may more effectively reveal subtle or undetectable dysregulations related to frailty at rest [3-5, 8]. A wearable ECG recording device provides an easy, practical solution for real-time cardiac signal recording and facilitates the quantification of autonomic responses during exercise. The PhysioNet dataset "Wearable-based signals during physical exercises from patients with frailty after open-heart surgery" offers a valuable resource for research in this domain [10]. The main goal of this paper is to evaluate whether frailty can be accurately assessed using HRV features combined with machine learning.

2. Data

This study used a PhysioNet database entitled "Wearable-based signals during physical exercises from patients with frailty after open-heart surgery" [10, 11]. This data includes synchronized single-lead ECG and triaxial acceleration signals from 80 older adults enrolled in a cardiac rehabilitation program after open-heart surgery, recorded during a sequence of standardized tests for health status assessment (veloergometry, six-minute walk, stair climbing, timed up and go, and treadmill gait analysis). A single-lead ECG recording was acquired using a Polar H10 wearable chest strap sensor with a sampling rate of 130 Hz [10, 11]. Frailty for each subject was assessed using the Edmonton Frail Scale (EFS), in which scores of 5 or lower were considered non-frail and scores of 6 or higher were considered frail. The number of available signals in each exercise in this study is summarized in Table 1. Only the six-minute walk test (6MWT) was used in this study for Frailty assessment.

3. Feature Extraction

QRS peaks were detected from the ECG signal during 6MWT using the Pan-Tompkins algorithm [12], followed by the extraction of 36 HRV features. Extracted features are grouped into six categories: statistical features, frequency features, traditional Poincare features, geometric Poincare features, heart rate asymmetry, and heart rate fragmentation.

Table 1. The Number of Available ECG Signals in Each Test

Tests	Number of Signals
Veloergometry	73
Six-Minute Walk	67
Stair Climbing	72
Timed Up and Go	75
Treadmill Gait Analysis	66

3.1. Statistical Features

With a finite number of intervals, consider RR intervals as RR_i with $i = 1, 2, ..., N$, where RR_i denotes the value of the i'th RR interval and N is the total number of successive intervals. The mean value of RR intervals (RR_mean) is the most evident of linear indexes of HRV [6]. Counting how many times each RR interval appears, *RR_mode* is the one that appears the most. *RR_median* is the middle value in a set of RR intervals. *RR_skew* is a measure of the asymmetry of the probability distribution of RR intervals about its mean, and *RR_kurt* refers to the distribution of data around the mean.

The standard deviation of RR intervals (SDRR) reflects the overall (both short-term and long-term) variation within the RR interval series, which is defined as:

$$SDRR = \sqrt{\frac{1}{N-1}\sum_{i=1}^{N}\left(RR_i - \overline{RR}\right)^2} \quad (1)$$

in which the mean RR interval is shown by $\overline{RR} = E\{RR_i\}$. The standard deviation of successive RR interval differences (SDSD) can be used as a measure of the short-term variability.

$$SDSD = \sqrt{E\left\{\Delta RR_i^2\right\} - E\left\{\Delta RR_i\right\}^2} \quad (2)$$

Another feature which is calculated from successive RR interval differences is the NN50, which is the number of successive intervals differing more than 50 ms:

$$pNN50 = \frac{NN50}{N-1} \times 100\% \quad (3)$$

3.2. Frequency Features

Very Low Frequency (VLF) power is a band of the power spectrum that ranges between 0.003 and 0.04 Hz, indicating overall activity of various slow mechanisms of sympathetic function. Low Frequency (LF) power is a band of the power spectrum that ranges from 0.04 to 0.15 Hz and measures both sympathetic and parasympathetic activity. High Frequency (HF) power, ranging from 0.15 to 0.4 Hz, reflects parasympathetic activity, and the LF/HF ratio indicates the overall balance between the sympathetic and parasympathetic systems [13].

3.3. Traditional Poincare Features

Poincare plot is a 2D space in which the pair of points is defined as: (RR_i, RR_{i+1}), in which $i = 1, 2, 3, ..., N-1$, *where* N is the number of *RR* intervals in the signal [14]. *SD1* and *SD2* are the standard descriptors of the Poincare plot that show the dispersion of points around the lines y = -x and $y = x$, respectively [15]. Tulppo et al. fitted an ellipse to the distribution of points in the Poincare plot [15] where *Cn* is the area of this estimated ellipse [16]. *CCM* is a descriptor introduced by Karmakar et al. that measures the temporal variation in the distribution of points in the Poincare plot [16].

3.4. Geometric Poincare Features

GOM and *COM* are defined by Moharreri et al., considering the points' location in relation to the line of identity [17]. Based on this definition, the points have three different positions in the Poincare plot: up, on, or down the line of identity [17]. Furthermore, they consider the location of two consecutive points in the Poincare plot to identify the dynamic behavior of points in this phase space [17].

3.5. Heart Rate Asymmetry (HRA)

HRA is defined based on the distribution of points above and below the identity line [18]. In HRA, the points above the line of identity are called deceleration, and the points below the line of identity are acceleration. *PI* is an index that shows the acceleration of the heart rate in relation to the points' distribution in the Poincare plot [19]. *GI* is the ratio of the distance of the points above the line of identity to the total distance of all points in Poincare space [20]. The *SI* index focused on the phase-angle difference between points above the line of identity [21].

3.6. Heart Rate Fragmentation (HRF)

HRF refers to irregularities and disruptions in heart rate patterns [22]. The Percentage of Inflection Points (PIP) is calculated as the combined percentage of transitions from HR acceleration to HR deceleration, or vice versa, and from HR acceleration/deceleration to stability (no change),

or vice versa [23]. The inverse of the average length of the acceleration/deceleration segments (IALS) is calculated by the inverse of the average number of ΔRR intervals in acceleration/deceleration segments, which are the sequence of RR intervals between consecutive inflection points for which the difference between two RR intervals is <0 and >0, respectively. The length of a segment is the number of RR intervals in that segment [22, 23]. The percentage of long segments (the number of ΔRR intervals in acceleration/deceleration segments with ≥3 ΔRR intervals over the total number of ΔRR intervals) is calculated, and its complement is the Percentage of Short Segments (PSS) [23]. The last feature in this field is the Percentage of RR Intervals in Alternation Segments (PAS). An alternation segment is a sequence of at least four RR intervals, for which heart rate acceleration changes sign every beat [22].

4. Model Development and Evaluation

To assess frailty, multiple classification models, including a decision tree and a neural network, were trained. Model performance was evaluated using a 5-fold cross-validation strategy, and the most effective classifier was selected based on cross-validated accuracy.

5. Results

Using EFS, 29 and 38 subjects were non-frail and frail, respectively. CatBoost was the most effective classifier in detecting Frailty, with an F1 score of 0.846 and an accuracy of 0.82. Additionally, this classifier achieved a precision and recall of 0.825 and 0.868, respectively. The confusion matrix, ROC curve, and precision-recall curve are shown in Figures 1, 2, and 3, respectively.

LF power, RR_mean, IALS, RR_mode, LF/HF ratio, PSS, and RR_skew were the top features identified using permutation-based importance that contributed to Frailty assessment.

Predicted / True	Non-frail	Frail	SUM
Non-frail	22 32.84%	7 10.45%	29 75.86% 24.14%
Frail	5 7.46%	33 49.25%	38 86.84% 13.16%
SUM	27 81.48% 18.52%	40 82.50% 17.50%	55 / 67 82.09% 17.91%

Figure 1. CatBoost confusion matrix for Frailty assessment

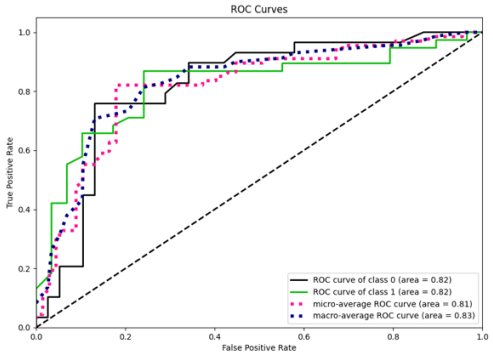

Figure 2. CatBoost ROC curve (class 0 and 1 are non-frail and frail, respectively). Area under the ROC curve for both non-frail and frail was 0.82.

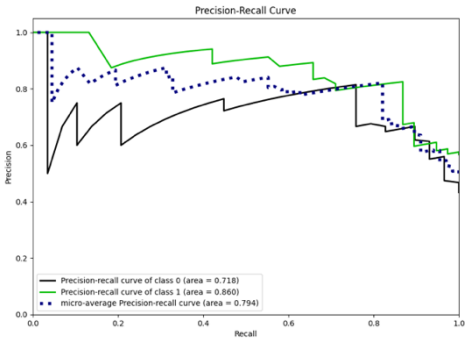

Figure 3. CatBoost precision-recall curve (class 0 and 1 are non-frail and frail, respectively). Area under the precision-recall curve for non-frail and frail was 0.718 and 0.86, respectively.

LF power and LF/HF ratio were selected as important features in the Catboost classifier, consistent with prior research reporting their importance for capturing impairment in cardiac ANS [24, 25]. Studies consistently show that heart rate fragmentation increases with age in both healthy subjects and individuals with coronary artery disease [26]. To the best of our knowledge, this is the first study to utilize heart rate fragmentation for frailty assessment, and our results indicate that HRF features (PSS and IALS) were important in frailty assessment.

In this study, pre-frail and frail individuals were grouped under a single 'frail' category due to the limited sample size. This limitation highlights the need to evaluate the proposed methodology on larger datasets that encompass all three frailty categories: non-frail, pre-frail, and frail. Furthermore, as the algorithm was developed using data from a single-center cohort, external validation on independent datasets is essential to assess the generalizability and robustness of the proposed frailty assessment approach.

References

[1] M. Pozzi *et al.*, "The frail patient undergoing cardiac surgery: lessons learned and future perspectives," *Frontiers in Cardiovascular Medicine,* vol. 10, 2023.

[2] M. A. Makary *et al.*, "Frailty as a predictor of surgical outcomes in older patients," *The American College of Surgeons,* vol. 210, pp. 901–908, 2010.

[3] S. Parvaneh *et al.*, "Regulation of cardiac autonomic nervous system control across frailty statuses: a systematic review," *Gerontology,* vol. 62, no. 1, pp. 3–15, 2015.

[4] K. Akbaş *et al.*, "Heart rate dynamics during localized upper-extremity function as a novel measure of cardiac autonomic dysfunction: investigation of aging-and disease-related alterations," *Gerontology,* vol. 71, no. 9, pp. 792–804, 2025.

[5] P. Arrué, K. Laksari, M. Russo, T. La Placa, M. Smith, and N. Toosizadeh, "Associating frailty and dynamic dysregulation between motor and cardiac autonomic systems," *Frontiers in Aging,* vol. 5, p. 1396636, 2024.

[6] E. Borell, J. Langbein, G. Despres, S. Hansen, C. Leterrier, and J. Forde, "Heart rate variability as a measure of autonomic regulation of cardiac activity for assessing stress and welfare in farm animals - a review," *Physiology & Behavior,* vol. 92, pp. 293–316, 2007.

[7] M. Eskandari, S. Parvaneh, H. Ehsani, M. Fain, and N. Toosizadeh, "Frailty identification using heart rate dynamics: a deep learning approach," *IEEE Journal of Biomedical and Health Informatics,* vol. 26, no. 7, pp. 3409–3417, 2022.

[8] N. Toosizadeh *et al.*, "Frailty and heart response to physical activity," *Archives of Gerontology and Geriatrics,* vol. 93, p. 104323, 2021.

[9] N. Toosizadeh, M. Eskandari, H. Ehsani, S. Parvaneh, M. Asghari, and N. Sweitzer, "Frailty assessment using a novel approach based on combined motor and cardiac functions: a pilot study," *BMC Geriatrics,* vol. 22, no. 1, p. 199, 2022. [Online].

[10] D. Sokas *et al.*, "Wearable-based Signals during Physical Exercises from Patients with Frailty after Open-Heart Surgery (version 1.0.0)," *PhysioNet,* 2022.

[11] A. L. Goldberger *et al.*, "PhysioBank, PhysioToolkit, and PhysioNet: Components of a New Research Resource for Complex Physiologic Signals," *Circulation,* vol. 101 (23), pp. 215–220, 2000.

[12] J. Pan and W. J. Tompkins, "A real-time QRS detection algorithm," *IEEE Transactions on Biomedical Engineering,* no. 3, pp. 230–236, 1985.

[13] S. Moharreri, S. Rezaei, N. Jafarnia Dabanloo, and S. Parvaneh, "Study of induced emotion by color stimuli: power spectrum analysis of heart rate variability," in *Computing in Cardiology (CinC2014)*, 2014, vol. 41, pp. 977–980.

[14] M. Brennan, M. Palaniswami, and P. Kamen, "Do existing measures of poincare plot geometry reflect nonlinear features of heart rate variability?," *IEEE Transactions on Biomedical Engineering,* vol. 48, no. 11, pp. 1342–1347, 2001.

[15] M. P. Tulppo, T. H. Makikallio, T. E. S. Takala, T. Seppanen, and H. V. Huikuri, "Quantitative beat-to-beat analysis of heart rate dynamics during exercise," *The American Journal of Physiology,* vol. 71, pp. 244 – 252, 1996.

[16] C. K. Karmakar, A. H. Khandoker, J. Gubbi, and M. Palaniswami, "Complex correlation measure: a novel descriptor for poincare plot," *Biomedical Engineering OnLine,* vol. 8, pp. 1–12, 2009.

[17] S. Moharreri, S. Parvaneh, N. Jafarnia Dabanloo, and A. M. Nasrabadi, "Utilizing occurrence sequence of heart rate's phase space points in order to discriminate heart arrhythmia," in *the 17th Iranian Conference of Biomedical Engineering (ICBME2010)*, Isfahan, Iran, 3–4 November 2010, vol. 17: IEEE.

[18] S. Parvaneh, N. Toosizadeh, and S. Moharreri, "Impact of mental stress on heart rate asymmetry," presented at *the Computing in Cardiology (CinC)*, 2015.

[19] A. Porta *et al.*, "Temporal asymmetries of short-term heart period variability are linked to autonomic regulation," *American Journal of Physiology-Regulatory, Integrative and Comparative Physiology,* vol. 295, no. 2, pp. R550–R557, 2008.

[20] J. Piskorski and P. Guzik, "Geometry of the poincaré plot of RR intervals and its asymmetry in healthy adults," *Physiological Measurement,* vol. 28, no. 3, p. 287, 2007.

[21] C. K. Karmakar, A. Khandoker, and M. Palaniswami, "Analysis of slope based heart rate asymmetry using poincare plots," presented at *the Computing in Cardiology (CinC),* 2012.

[22] M. D. Costa, R. B. Davis, and A. L. Goldberger, "Heart rate fragmentation: a new approach to the analysis of cardiac interbeat interval dynamics," *Frontiers in Physiology,* vol. 8, 2017.

[23] Y. Sawayama *et al.*, "Heart rate fragmentation, ambulatory blood pressure, and coronary artery calcification: a population-based study," *JACC: Asia,* vol. 4(3), pp. 216–225, 2024.

[24] L. Álvarez-Millán *et al.*, "Chronotropic response and heart rate variability before and after a 160 m walking test in young, middle-aged, frail, and non-frail older adults," *International Journal of Environmental Research and Public Health,* vol. 19, no. 14, p. 8413, 2022.

[25] R. Varadhan *et al.*, "Frailty and impaired cardiac autonomic control: new insights from principal components aggregation of traditional heart rate variability indices," *Journals of Gerontology Series A: Biomedical Sciences and Medical Sciences,* vol. 64, no. 6, pp. 682–687, 2009.

[26] M. D. Costa, S. Redline, T. M. Hughes, S. R. Heckbert, and A. L. Goldberger, "Prediction of cognitive decline using heart rate fragmentation analysis: The multi-ethnic study of atherosclerosis," *Frontiers in Aging Neuroscience,* vol. 13, p. 708130, 2021.

Address for correspondence:
Saman Parvaneh
1 Edwards Way, Irvine, CA, USA
parvaneh@ieee.org